Cretaceous Research 141 (2023) 105367

Contents lists available at ScienceDirect

Cretaceous Research

journal homepage: www.elsevier.com/locate/CretRes

# Dinoflagellate cysts from the Upper Cretaceous (Campanian–Maastrichtian) from The Naze Peninsula, James Ross Island, Antarctica

Luis-Andrés Guerrero-Murcia [a, *], Javier Helenes [a], Mercedes di Pasquo [b], James Martin [c]

[a] Departamento de Geología, Centro de Estudios Científicos y de Educación Superior de Ensenada, Carretera Ensenada-Tijuana No. 3918, Fracc. Zona Playitas, CP 22860, Ensenada, B.C., Mexico
[b] Consejo de Investigaciones Cientificas y Tecnológicas (CONICET), Laboratorio de Palinoestratigrafía y Paleobotánica, CICyTTP-CONICET, Dr. Matteri y España, Diamante, CP E3105BWA, Entre Ríos, Argentina
[c] School of Geosciences, University of Louisiana, Lafayette, LA, 70504, USA

ARTICLE INFO

*Article history:*
Received 17 May 2022
Received in revised form
12 September 2022
Accepted in revised form 12 September 2022
Available online 18 September 2022

*Keywords:*
Dinoflagellates cysts
Biostratigraphy
Paleoecology
Antarctic Peninsula
Paleoproductivity

ABSTRACT

We present the results of the quantitative and qualitative study of dinoflagellate cysts in outcrop samples from a section of the Snow Hill Island Formation (SHF) in James Ross Island, Antarctic. Dinoflagellate cysts assemblages are abundant and dominated by gonyaulacoid taxa. The last occurrence of the dinoflagellate cyst *Kallosphaeridium? helbyi* and *Chatangiella granulifera*, together with the first occurrence of *Pterodinium cretaceum*, indicates a probable late Campanian age (~76.4–~72.1 Ma) for the lower strata. Whereas the first occurrence of *Manumiella bertodano* and the last occurrence of *Odontochitina operculata, Xenascus ceratioides,* and *Stiphrosphaeridium anthophorum* indicate an early Maastrichtian (~72.1–~70.0 Ma) age for the upper strata. Our results, combined with paleobotanical and palynological published data, indicate medium–high continental and marine productivity with temperate paleoclimate free of glaciers for this interval. Lithological and paleontological data indicate mainly inner neritic marine depositional environments. The predominance of shales in the lower part of the lower Maastrichtian interval indicates a slightly deeper environment. In contrast, in the middle part of the lower Maastrichtian, a shallower, transitional environment is marked by the presence of theropod dinosaurs and decapod crustaceans.



## 1. Introduction

Knowledge of the Antarctic Peninsula is essential to improve our understanding of the Antarctic continent's geological evolution and its relationship with the rest of the surrounding continents. James Ross Island is located to the northeast of the Antarctic Peninsula, and within the Island, The Naze Peninsula (Fig. 1) contains outcrops of Upper Cretaceous sediments belonging to the Cape Lamb Member (CLM) of the Snow Hill Island Formation, Marambio Group. A Campanian–Maastrichtian assignment of the CLM, is indicated by chronostratigraphic and absolute dating analyses carried out in correlative strata from Cape Lamb, Vega Island (Crame et al., 1999, 2004). Since we are dealing exclusively with The Naze Peninsula in this paper, we will refer to this locality as The Naze, where macro and microfossil data (Guerra et al., 2015; Amenábar et al., 2019; Piovesan et al., 2020), reveal a Campanian-early Maastrichtian age, while palynological data from the CLM indicate a Campanian (Askin, 1988) and early Maastrichtian age for the entire section (di Pasquo and Martin, 2013). In contrast, a dinoflagellate cyst zonation based on Seymour Island (Bowman et al., 2012) considers the CLM not older than early Maastrichtian.

Additionally, paleoclimatic evidence indicates a cool-temperate climate, free of glaciers with high rainfall conditions during the Maastrichtian (Dettmann, 1986, 1989; Askin, 1990a, 1990b; Dettmann et al., 1992; Crame, 1992; Hill and Scriven, 1995; Miller et al., 2008; Friedrich et al., 2009; Bastos et al., 2013). Afterward,

* Corresponding author. Departamento de Geología, Centro de Estudios Científicos y de Educación Superior de Ensenada, Carretera Ensenada-Tijuana No. 3918, Fracc. Zona Playitas, CP 22860, Ensenada, B.C., Mexico.
*E-mail addresses:* lguerrero@cicese.edu.mx (L.-A. Guerrero-Murcia), jhelenes@cicese.mx (J. Helenes), medipa@cicyttp.org.ar (M. di Pasquo), jxm2118@louisiana.edu (J. Martin).

https://doi.org/10.1016/j.cretres.2022.105367
0195-6671/

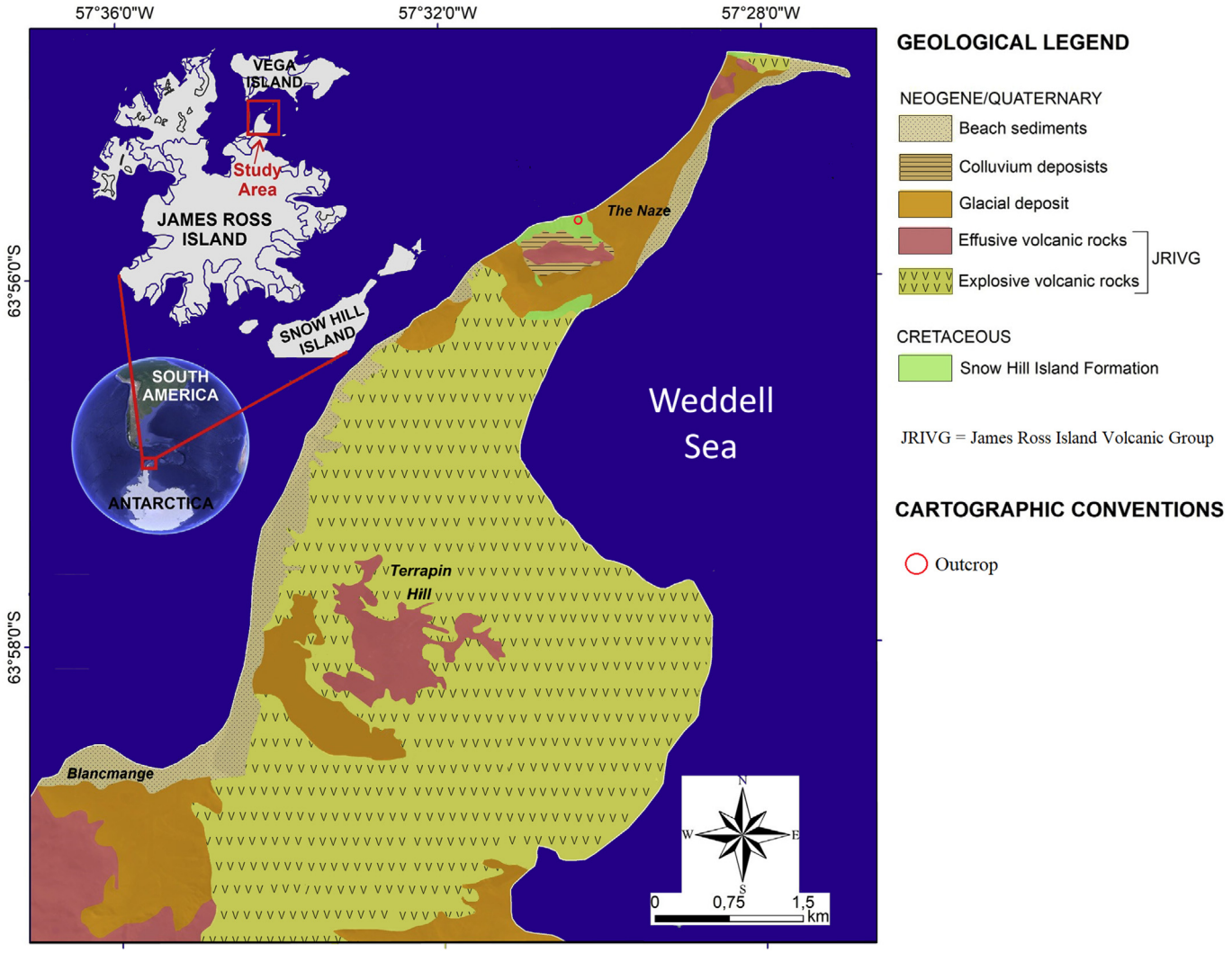


**Fig. 1.** Location of James Ross Island, The Naze Peninsula, and outcrop studied (modified from Piovesan et al., 2020).

the appearance of glaciers was interpreted in the Antarctic Peninsula during the Maastrichtian–Danian (Bowman et al., 2012, 2014), when this region formed a southern polar province separated from South America.

According to lithology, benthic foraminifera, palynomorphs, and megafossils, the strata of The Naze were deposited in low-energy shelf settings (Olivero, 2012; di Pasquo and Martin, 2013; Guerra et al., 2015; Piosevan et al., 2020).

We document the dinoflagellate cyst assemblages to determine the age of the CLM cropping out at The Naze. Analyses of these assemblages point out the environmental and paleoecological signals preserved in the strata studied. Integration of this data with published information on lithology and paleontology (di Pasquo and Martin, 2013) will also help determine the region's paleoclimatic conditions. A discussion on the age of these strata is included, supported by the dinoflagellate cyst taxa documented.

## 2. Materials and methods

This study includes the preparation and analyses of 47 samples from a 90 m thick section of the Cape Lamb Member of the Snow Hill Island Formation, cropping out in The Naze. These samples belong to the repository C18 Antarctica, J.R.I. of the Centro de Investigación Científica y de Educación Superior de Ensenada (CICESE), Ensenada, Baja California, Mexico (Appendix A, supplementary online material). The base of the section is at sea level, and at the top, there is a Miocene basalt sill (Calabozo et al., 2015). The lithology (Fig. 2) is dominated by fine-grained, laminated to massive, green–gray sandstones, interspersed with yellow–green mudstone and clayey-siltstones, containing calcareous concretions and layers of bentonite (di Pasquo and Martin, 2013). This section contains the remains of a theropod paravian dinosaur and several vertebrates (Martin et al., 2007; Case et al., 2007). Ely and Case (2019) described the paravian dinosaur collected at approximately 45 m of the base (red arrow; Fig. 2). There are no reports of discontinuities in this section.

### 2.1. Sampling and palynological processing

The samples were collected between the basal 3.42 m (sample AC-2) and the upper 81.73 m (sample AC-48), covering a total thickness of 78.31 m (Fig. 2). The samples were processed according to the methodology described in Wood et al. (1996) but without oxidation to avoid specimen destruction (Mertens et al., 2009). A spore tablet of *Lycopodium clavatum* (Batch 124961 = 12,542 spores) was added to each sample to evaluate the concentration of palynomorphs per gram of sediment (Benninghoff, 1962). The complete processing included eliminating carbonates with

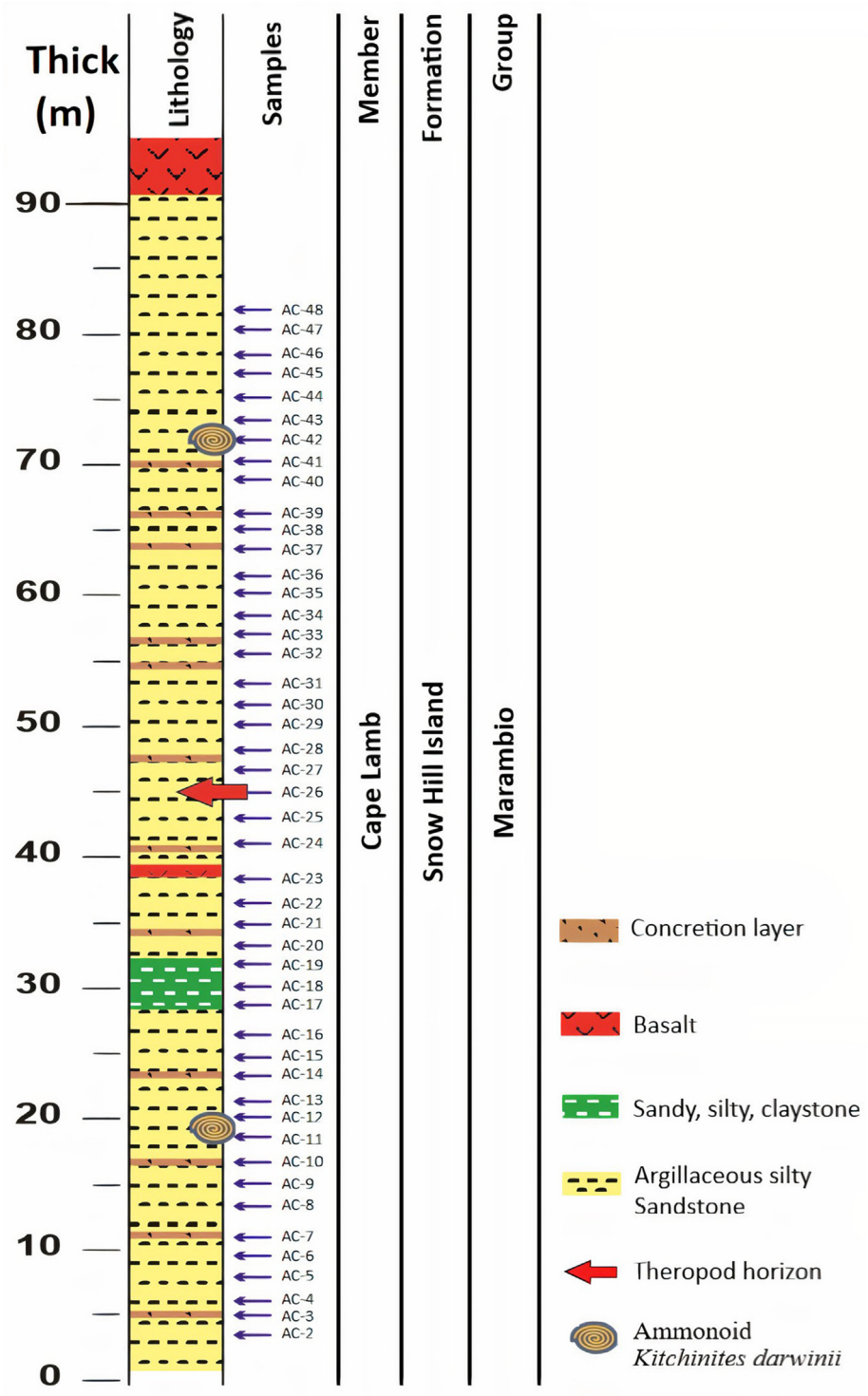


**Fig. 2.** Stratigraphic section of the outcrop at The Naze Peninsula, with lithology, the vertical scale in meters (m), and the 47 samples (AC-2 to AC-48) analyzed in the present study (modified from di Pasquo and Martin, 2013).

hydrochloric acid (HCl) and silicates with hydrofluoric acid (HF). Then, we separated the organic from the residue with sodium polytungstate ($Na_6$ [$H_2W_{12}O_6$]; sp. gr. = 2.0), and finally, after cleaning and sieving, the residue was mounted for microscope analysis. Seven to ten drops of the residue were collected and mounted on a 25 × 50 mm coverslip with glycerin jelly. The 47 slides were examined using a transmitted light optical microscope (Olympus CX31), with magnifications of 200×, 400×, and 1000×. The total of *L. clavatum* was used as an exotic marker, and the sum of dinoflagellate cysts was counted. The taxonomic classification of dinoflagellate cysts follows Fensome (2019) conventions. Since this study includes only organic-walled, acid-resistant hypnozygotic cysts of dinoflagellates, we refer to them as dinoflagellate cysts hereafter.

The concentration of dinoflagellate cysts per gram of sediment (cyst/g sed) was calculated using the method proposed by Maher (1981); Mertens et al. (2009, 2012). As a proxy of marine productivity (Harland, 1973; Reichart and Brinkhuis, 2003) we estimated a Heterotrophic–Autotrophic concentration index (H–A, Equation (1)). The Shannon diversity index (H) was calculated to evaluate each abundance and equity of species in each sample (Shannon and Weaver, 1949).

$$H{-}A = \left(\frac{HC}{HC + AC}\right) * 100 \quad (1)$$

where, Heterotrophic–autotrophic concentration index. HC = heterotrophic concentration; AC = Autotrophic Concentration.

### 2.2. Statistical analysis

We performed a Principal Component Analysis (PCA) to simplify our database and identify the most consistent species. First, we selected taxa with a significative Pearson correlation ($r \geq 0.50$) and a 95% confidence level, with average relative abundances >1%, and present in >60% of the samples analyzed. The PCA was made with the logarithmic values of the 'dinoflagellates' cyst normalized concentrations to ensure that each species or taxonomic group contributes equally to the multivariate analysis.

## 3. Geological and paleoecological framework

The Upper Cretaceous sedimentary sequence in the James Ross Basin area includes the Santonian?–Maastrichtian Marambio Group, which consists of marine clastic sediments with a diverse and abundant mega fossil fauna and flora (Crame et al., 1999, 2004). This group is subdivided into the Santa Marta (Santonian? to Campanian), Snow Hill Island (Campanian to Maastrichtian), and López de Bertodano (Maastrichtian) formations (Fig. 3).

The general stratigraphic distribution of some dinoflagellates cysts in the Snow Hill and López-Bertodano formations is known (Askin, 1988; Crame et al., 1991; Pirrie et al., 1991) and support a palynological biozonation scheme for the late Maastrichtian to early Danian interval in Antarctica (Bowman et al., 2012), for which the detailed morphological analysis of the genus *Manumiella* (Thorn et al., 2009) is advantageous. This zonation includes three Maastrichtian zones, three subzones, and one Danian zone.

The Campanian–Maastrichtian (Cam–Maas) boundary has been recognized by megafossil evidence on Vega Island (Crame et al., 1999, 2004) and on Seymour Island (Askin, 1988), also by recordings of macro and microfossils (Guerra et al., 2015; Amenábar et al., 2019) but it is poorly defined with dinoflagellate cysts. At the Naze, this Cam–Maas boundary has been reported by Piosevan et al. (2020) based on foraminifera. Correlative strata assigned to the López de Bertodano Formation were assigned a Campanian age (Crame et al., 1991). Di Pasquo and Martin (2013) carried out the first palynological analysis of 16 samples from the section studied in the present work that revealed diverse assemblages composed of 100 relatively well-preserved species. The principal terrestrial groups (32%) are represented by lycophytes (8 species), pteridophytes (15 species), gymnosperms (13 species), angiosperms (21 species), and freshwater chlorococcaleans (3 species). Marine palynomorphs (68%) belong to dinoflagellates (61 species), chlorococcaleans (6 species), and one acritarch. The vertical distribution of selected species allowed the distinction of two informal assemblages: the lower *Odontochitina porifera* assemblage from the base to its appearance in the lower part of the section. The *Batiacasphaera grandis* assemblage characterizes the remaining section. A variable abundance of the heterotrophic genera *Manumiella* and *Isabelidinium* was documented across this section. An early Maastrichtian age proposed for this section based on the global stratigraphic ranges of selected palynomorphs is also supported by the ammonoid *Kitchinites darwinii*, up to ~19 m from the bottom of the section. Concerning the regional paleoecological conditions, the presence of gymnosperm pollen from the family Podocarpaceae, together with *Nothofagus* and other angiosperms (di Pasquo and Martin, 2013), supports a cool-temperate climate, free of frost (Dettmann, 1986, 1989; Askin, 1990a, 1990b; Crame, 1992; Hill and Scriven, 1995; Bowman et al., 2013a,b; Linnert et al., 2018). The presence of spores of aquatic ferns and mosses, characteristic of marshes or wetlands, indicates high rainfall during the later Cretaceous in the Antarctic Peninsula. The upper Campanian to Maastrichtian palynological associations of Seymour Island (Askin, 1990a, 1990b), east of James Ross Island, also indicates a rainforest dominated by Podocarpaceae. In this area, angiosperm pollen and low diversity of cryptogam spores developed in a cool to temperate-warm place and confirm that the Campanian–Maastrichtian interval was a relatively temperate interval with stable wet paleoclimate.

Comparison of the assemblages of dinoflagellate cysts observed here, with the record of relative abundance of pollen and spores of the 16 samples studied by di Pascuao and Martin (2013) indicates the predominance of marine conditions. Dinoflagellate cysts are more abundant (>70%) than continental palynomorphs throughout the sedimentary column, while gymnosperm pollen represent the most abundant continental group along the column, followed by angiosperm pollen and spores.

The genus Nothofagidites (Dettmann, 1989) is the most abundant within the angiosperm Fagaceae reported in samples from The Naze. The genus has been recognized since the Campanian, and it is abundant and diverse in the Maastrichtian of the Antarctic Peninsula, where it has been associated with ice-free areas (Haller, 2002). The common presence of this taxon throughout the entire sedimentary column includes representatives of the Fusca group (*Nothofagidites saraensis*), the Brassii group (*Nothofagidites dorotensis*), and the Menziesii group (*Nothofagidites americanus*). The presence of the Fusca group is significant because it indicates moderate effective humidity and temperate climates (Barreda, 1997).

On the marine record, the presence of endemic species of dinoflagellates (*Operculodinium exilicornutum*, and *Batiacasphaera grandis*) in the James Ross Basin allows the proposal of a polar southern province separated from South America during the Maastrichtian and Danian (Bowman et al., 2012; di Pasquo and Martin, 2013). The similarity of high latitude dinoflagellate cysts associations and the correlation with models of ocean currents around Antarctica allows the recognition of this province in New Zealand, southern Australia, and the southwestern coast of South America, with an oceanic connection between southern South America and the Tasman Sea through Antarctica, for the Maastrichtian–Danian interval. The paleoecological importance of dinoflagellates has been studied and related more profusely with environmental changes associated with the Cretaceous/Paleogene boundary on Marambio (Thorn et al., 2009), Vega and Seymour (Bowman et al., 2012, 2013a,b) islands. In those areas, a high abundance of the heterotrophic genera *Manumiella* and *Isabelidinium* below the Cretaceous/Paleogene limit was associated with short-term marine regressions and oceanic cooling events that occurred before the extinction of several dinoflagellate taxa around across this limit.

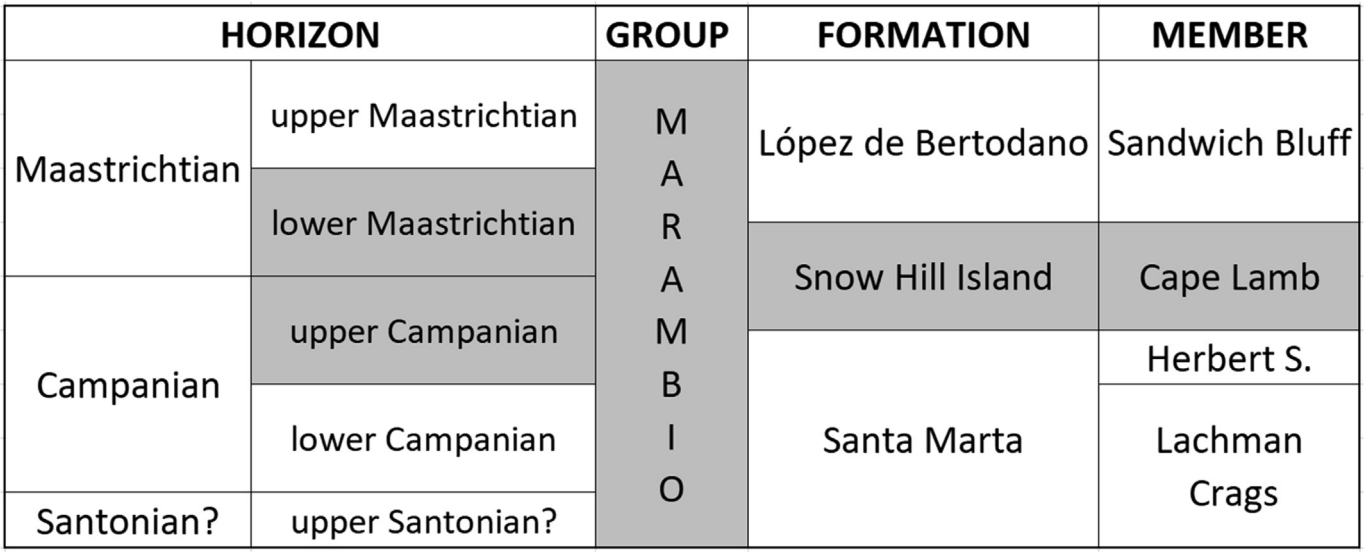


**Fig. 3.** Upper Cretaceous Stratigraphy scheme in the James Ross Basin. Taken and modified from Piosevan et al. (2020). The Cape Lamb Member of the Snow Hill Formation is the unit analyzed in this paper.

## 4. Results

### 4.1. Basic statistics and taxonomy

Recovery was good to excellent, with an average of 680 specimens per sample representing 49 dinoflagellate cyst taxa (Appendix B, supplementary online material). The cyst assemblages are slightly dominated by the gonyaulacoid forms, with an average of 363 specimens against 268 peridinioid forms. However, the sample AC-26 is unusual because it contains 3402 specimens of the gonyaulacoid *Cribroperidinium muderongense*. In general, the counts of *C. muderongense* (mean = 236.3) are the highest of all the taxa observed, with the recovery of more than 1000 specimens in two other samples (AC-36 = 1199; AC-34 = 1204). The abnormally high value from sample AC-26 probably reflects a closer shoreline, as some researchers (Slimani et al., 2019) suggest that *C. muderongense* indicates deposition in inner neritic marginal environments. This nearshore condition would explain the higher terrigenous influx evidenced by the theropod dinosaur remains reported in the same interval (di Pasquo and Martin, 2013). The average count of *C. muderongense* in the two adjacent samples is 260, which is an atypically large count. We calculated all our concentrations and statistical parameters with the original counts but kept this unusual data for our interpretations (see Table 1).

We consider that the similarity of the tabulation patterns indicates the trophic strategies of the taxa found. In particular, the areoligerioid taxa (Areo), known to have a completely gonyaulacoid paratabulation pattern, including the lack of anterior intercalary paraplates, and the gonyaulacoid distribution of the postcingular series, is believed here to represent an autotrophic group. On the other hand, the cretaceous ceratioide forms observed are similar to

**Table 1**
Basic statistics of dinoflagellate cyst counts and concentrations in samples from The Naze. The green shaded boxes indicate autotrophic taxa, while the brown indicate heterotrophic taxa. Param = parameter; Max = maximum value; Min = minimum value; St Dev = standard deviation.

| Param | Counts | | | | |
|---|---|---|---|---|---|
| | Gony | Areo | Peri | Cera | Total |
| Mean | 363 | 3 | 268 | 45 | 680 |
| Max | 3,898 | 43 | 814 | 381 | 4,042 |
| Min | 36 | 0 | 50 | 0 | 132 |
| St Dev | 621 | 7 | 192 | 82 | 696 |
| | Concentration (cyst/g sed) | | | | |
| Mean | 886.4 | 5.9 | 538.7 | 78.0 | 1,430.9 |
| Max | 16,835.0 | 56.6 | 2,509.3 | 580.8 | 17,456.9 |
| Min | 55.3 | 0.0 | 89.1 | 0.0 | 157.0 |
| St Dev | 2,449.3 | 11.6 | 459.6 | 127.9 | 2,559.3 |

**Table 2**
Richness (Number of species) and relative abundance in percentages of dinoflagellate cysts from The Naze. The green shaded boxes indicate autotrophic taxa, while the brown indicates heterotrophic taxa.

| Families | Richness (%) | Relative Abund (%) |
|---|---|---|
| Gonyaulacaceae | 14 (28.57) | 53.44 |
| Areoligeraceae | 3 (6.12) | 0.41 |
| Peridiniaceae | 27 (55.10) | 39.46 |
| Ceratiaceae | 5 (10.20) | 6.69 |

**Table 3**
Basic statistics of trophic groups Aut = autotrophic; Het = heterotrophic; TOT = total sum of dinoflagellate cysts; Het–Aut = heterotrophic–autotrophic index; Div (H) = Shannon diversity index. Param = parameter; Max = maximum value; Min = minimum value; St Dev = standard deviation.

| Param | Aut | Het | TOT | Het–Aut | Div (H) |
|---|---|---|---|---|---|
| Mean | 892.3 | 616.6 | 1508.9 | 0.54 | 3.34 |
| Max | 16,835.0 | 2527.6 | 17,456.9 | 0.88 | 4.77 |
| Min | 58.2 | 92.6 | 318.0 | 0.04 | 1.01 |
| St Dev | 2422.0 | 469.7 | 2524.1 | 0.18 | 0.66 |

the living *Ceratium*, so they are interpreted as heterotrophic. Hence, we consider 17 autotrophic (Aut) taxa (Gony and Areo) and 32 heterotrophic (Het) taxa (Peri and Cera) (Table 2).

The more diverse heterotrophic group is not the more abundant one since the 27 peridinioid species observed represent 39.46% of the total abundance, while the 14 gonyaulacoid species represent 53.44% of the total abundance (Table 2).

Among the identified 49 cyst species, 27 belong to the Peridiniacean (Peri) family, 14 belong to the Gonyaulacaceae (Gony), 5 are Ceratiacean (Cera), and 3 are Areoligeracean (Areo). To try to understand the behavior of the different types of dinoflagellates represented in our study, we assembled them into autotrophic (Aut) and heterotrophic (Het) groups (Table 3) and calculated the Het–Aut index and the Shannon Diversity Index (H). The mean concentration of total dinoflagellates is 1508.88 cyst/g sed, with Aut = 892.27 cyst/g sed and that of Het = 616.62 cyst/g sed. The mean Het–Aut Index = 0.54 indicates a minor predominance of Het.

#### 4.1.1. PCA grouping

For the PCA, the following 15 species *Cribroperidinium muderongense, Operculodinium radiculatum, Manumiella seymourensis, Isabelidinium cretaceum, Spiniferites ramosus, Xensacus plotei, Manumiella druggii, Manumiella seelandica, Isabelidinium papillum, Isabelidinium cooksoniae, Isabelidinium pellucidum, Isabelidinium belfastense, Operculodinium centrocarpum, Palaeocystodinium*

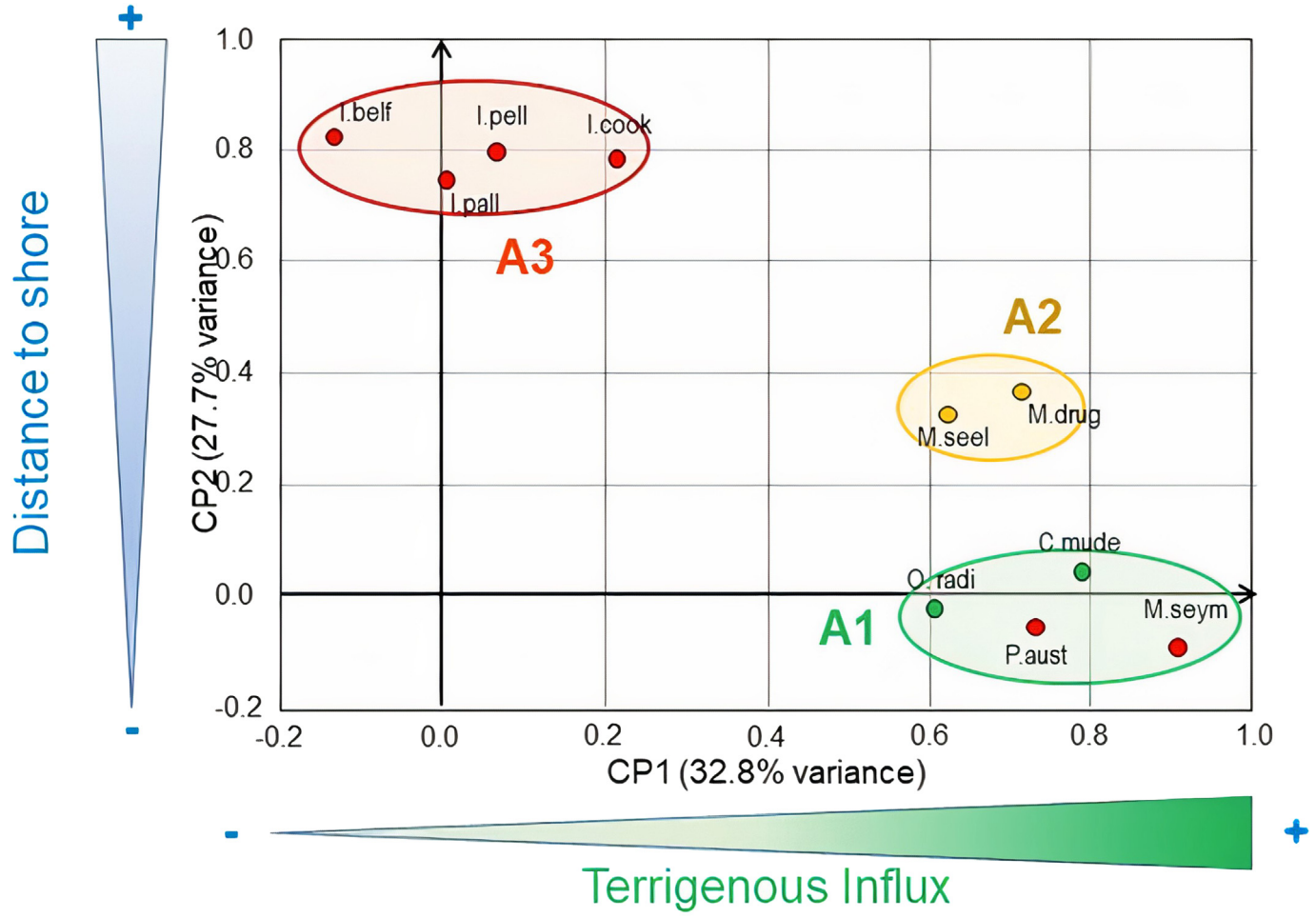


**Fig. 4.** Ordination diagrams generated from PCA performed on log-transformed and normalized dinoflagellate cyst concentrations. Taxa included in Groups A1 (green) integrated by mostly Aut and some Het, A2 (orange), and A3 (red) composed exclusively by Het taxa. (For interpretation of the references to color in this figure legend, the reader is referred to the Web version of this article.)

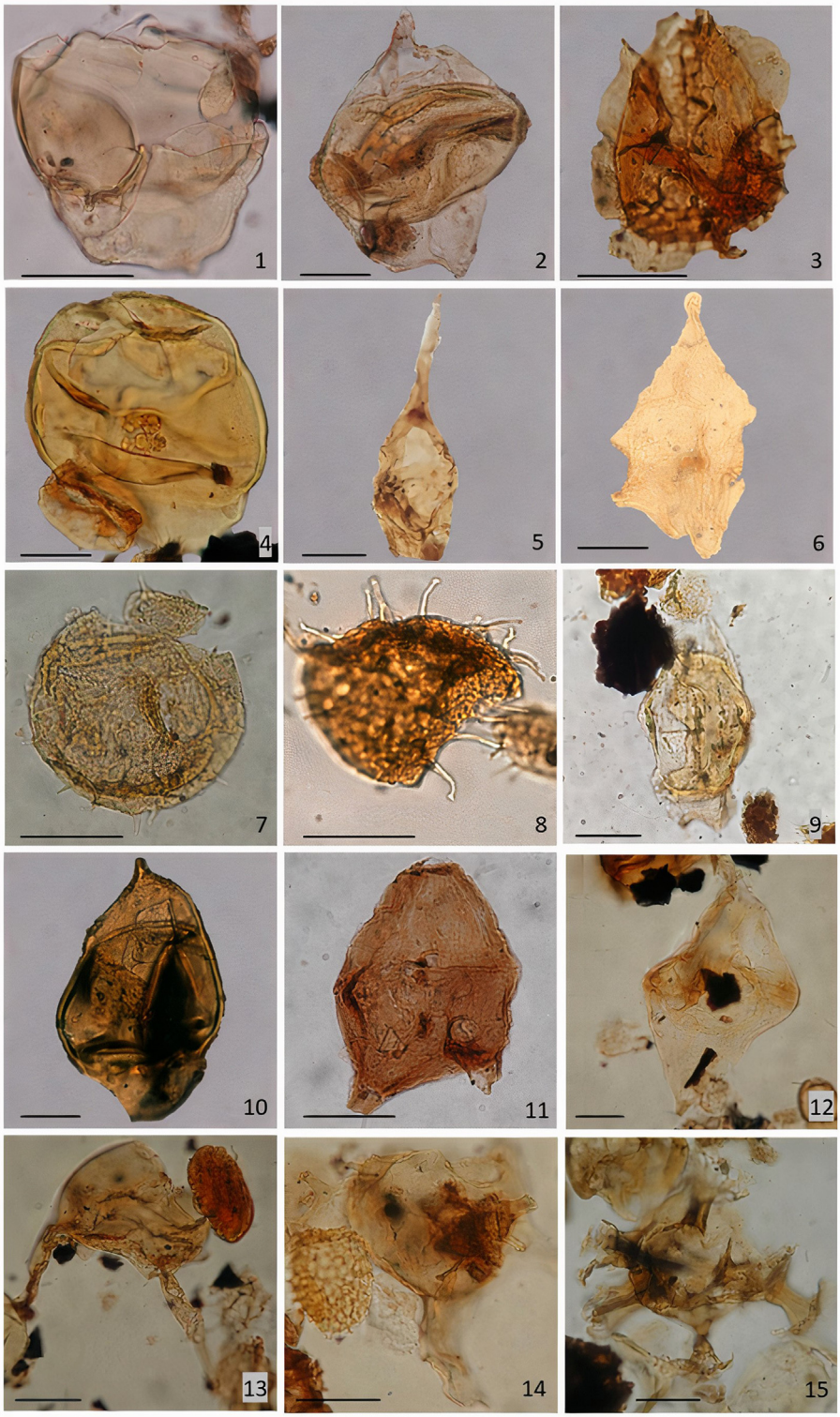


**Fig. 5.** Marker species pictures in this work; all images were taken with Olympus CX31 microscope at palynology laboratory of CICESE. The illustrations are shown following the biostratigraphic order used for the present study's analysis. 1: *Kallosphaeridium? Helbyi*, Repository (R): C18-Ant. J.R.I AC-9, Outcrop Level (OL): 14.97 m, England Finder (EF): W64/1, Slide Magnification (SM): 1000×, Scale Bar (SB): 30 μm; 2: *Chatangiella granulifera*, R: C18-Ant. J.R.I AC-11, OL: 18.57 m, EF: U44/2, SM: 1000×, SB: 30 μm; 3: *Pterodinium cretaceum*, R: C18-Ant. J.R.I AC-25, OL: 44.90 m, EF: X47/2, SM: 1000×, SB:30 μm; 4: *Manumiella seymourensis*, R: C18-Ant. J.R.I AC-2, OL: 3.42 m, EF: Q25/4, SM: 1000×, SB: 30 μm; 5: *Palaeocystodinium australinum*, R: C18-Ant. J.R.I AC-38, OL: 64.96 m, EF: E14/2, SM: 1000×, SB: 30 μm; 6: *Canninginopsis ordospinosa*, R: C18-Ant. J.R.I AC-21, OL: 34.75 m, EF: K69/2, SM: 400×, SB: 30 μm; 7: *Operculodinium flucturum*, R: C18-Ant. J.R.I AC-10, OL: 16.64 m, EF: W28/3, SM: 1000×, SB: 30 μm; 8: *Operculodinium radiculatum*, R: C18-Ant. J.R.I AC-2, OL: 3.42 m, EF: D26/4, SM: 1000×, SB: 30 μm; 9: *Chatangiella campbellensis,* R: C18-Ant. J.R.I AC-5, OL: 7.83 m, EF: D28/0, SM: 1000×, SB: 30 μm; 10: *Isabellidinium papillum*, R: C18-Ant. J.R.I AC-3, OL: 4.93 m, EF: D21/4, SM: 1000×, SB: 30 μm; 11: *Octodinium askiniae*, R: C18-Ant. J.R.I AC-42, OL: 71.82 m, EF: Y18/0, SM: 1000×, SB: 30 μm; 12: *Manumiella bertodano*, R: C18-Ant. J.R.I AC-25, OL: 42.92 m, EF: K69/2, SM: 1000×, SB: 30 μm; 13: *Odontochitina operculata*, R: C18-Ant. J.R.I AC-5, OL: 7.83 m, EF: X26/4, SM: 1000×, SB: 30 μm; 14: *Xenascus ceratioides*, R: C18-Ant. J.R.I AC-48, OL: 81.73 m, EF: W43/3, SM: 1000×, SB: 30 μm; 15: *Stiphrosphaeridium anthophorum*, R: C18-Ant. J.R.I AC-14, OL: 23.19 m, EF: B62/3, SM: 1000×, SB: 30 μm.

*australinum*, and *Palaeocystodinium lidiae* satisfied the requisites mentioned at point 2.2. However, only ten species remain for the final analysis when performing the correlation matrix. Results of PCA indicate that two components (Fig. 4), PC1 (32.81%) and PC2 (27.74%), explain 60.55% of the variance. PC2 determines two different groups, the first group A1, includes the most common and abundant Aut taxa, together with the Het *P. australinum* and *M. seymourensis*. The second group, A2, includes the Het *M. druggii* and *M. seelandica*. In contrast, PC1 establishes only one compact Het Group A3, with *I. papillum, I. cooksoniae, I. pellucidum,* and *I. belfastense*.

This binary distribution indicates the direct influence of two factors. The Het Group A1 has very high values along Axis 1 and very low on Axis 2. In contrast, Het Group A2 has very high values along Axis 2 and very low on Axis 1, with Aut Group A3, which is dominated by the most abundant Aut taxa. Het taxa characterize recent assemblages from highly productive areas with coastal upwelling conditions, while an abundance of Aut taxa is usually found in nearshore areas (Vink et al., 2000), where there can be significant terrigenous influx. Therefore, our PCA's twofold spreading represents marine productivity associated with terrigenous influx along Axis Fig. 1, whereas Axis 2 probably reflects coastal upwelling conditions.

### 4.2. Biostratigraphy

The stratigraphic distribution found in the literature of 15 of the 49 identified dinoflagellate cyst species (Fig. 5) allows for establishing a chronostratigraphic framework for the column studied (Fig. 6). Thirty-eight of the species observed at The Naze Peninsula have their first records at ages older than late Campanian, but most of their reported stratigraphic ranges include the Maastrichtian in agreement with di Pasquo and Martin (2013).

The lower samples of the outcrop contain nine species that appeared during the upper Campanian (Davey, 1969; Wilson, 1984; Bujak and Williams, 1985; Askin et al., 1991; Smith, 1992; Pirrie et al., 1997; Roncaglia et al., 1999; Askin, 1999; Brinkhuis et al., 2003; Slimani et al., 2008; di Pasquo and Martin, 2013). These are *Pterodinium cretaceum*, *Manumiella seymourensis*, *Palaeocystodinium australinum*, *Canningia ordospinosa*, *Operculodinium flucturum*, *Operculodinium radiculatum*, *Chatangiella campbellensis*, *Isabelidinium papillum*, and *Octodinium askiniae*. Additionally, these same strata also contain *Chatangiella granulifera* and *Kallosphaeridium? helbyi*, which have their last records at the Campanian/Maastrichtian limit (Bujak and Williams, 1985, in Mao and Mohr, 1992; Helenes and Somoza, 1999), indicating that the oldest layers were deposited probably in the upper Campanian (Fig. 7).

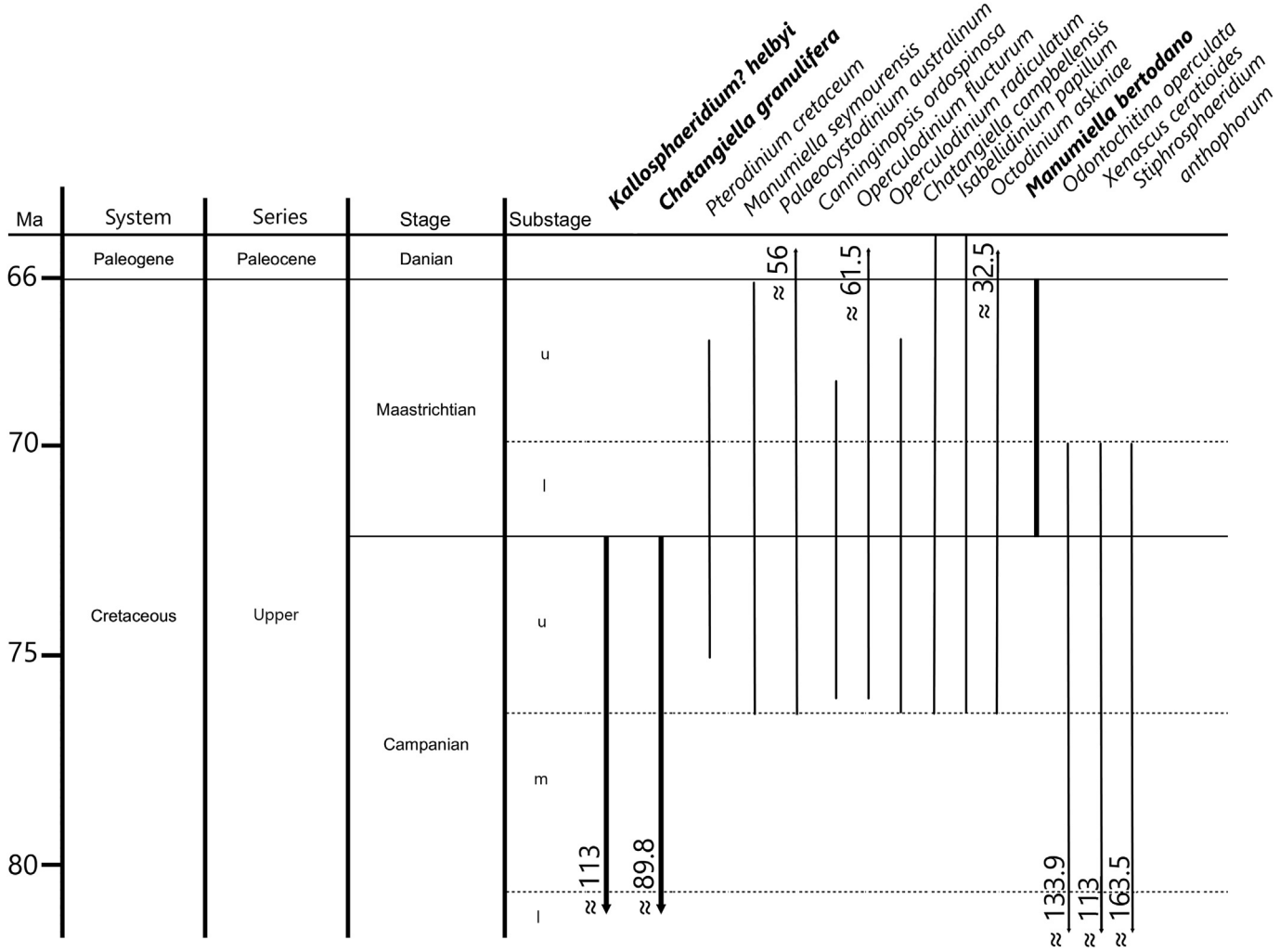


**Fig. 6.** Reported range of upper Campanian and lower Maastrichtian marker species. The three index species are in bold, and their stratigraphic distribution is highlighted with heavier lines. l = lower, m = middle, u = upper. The age scale corresponds to Gradstein et al. (2012).

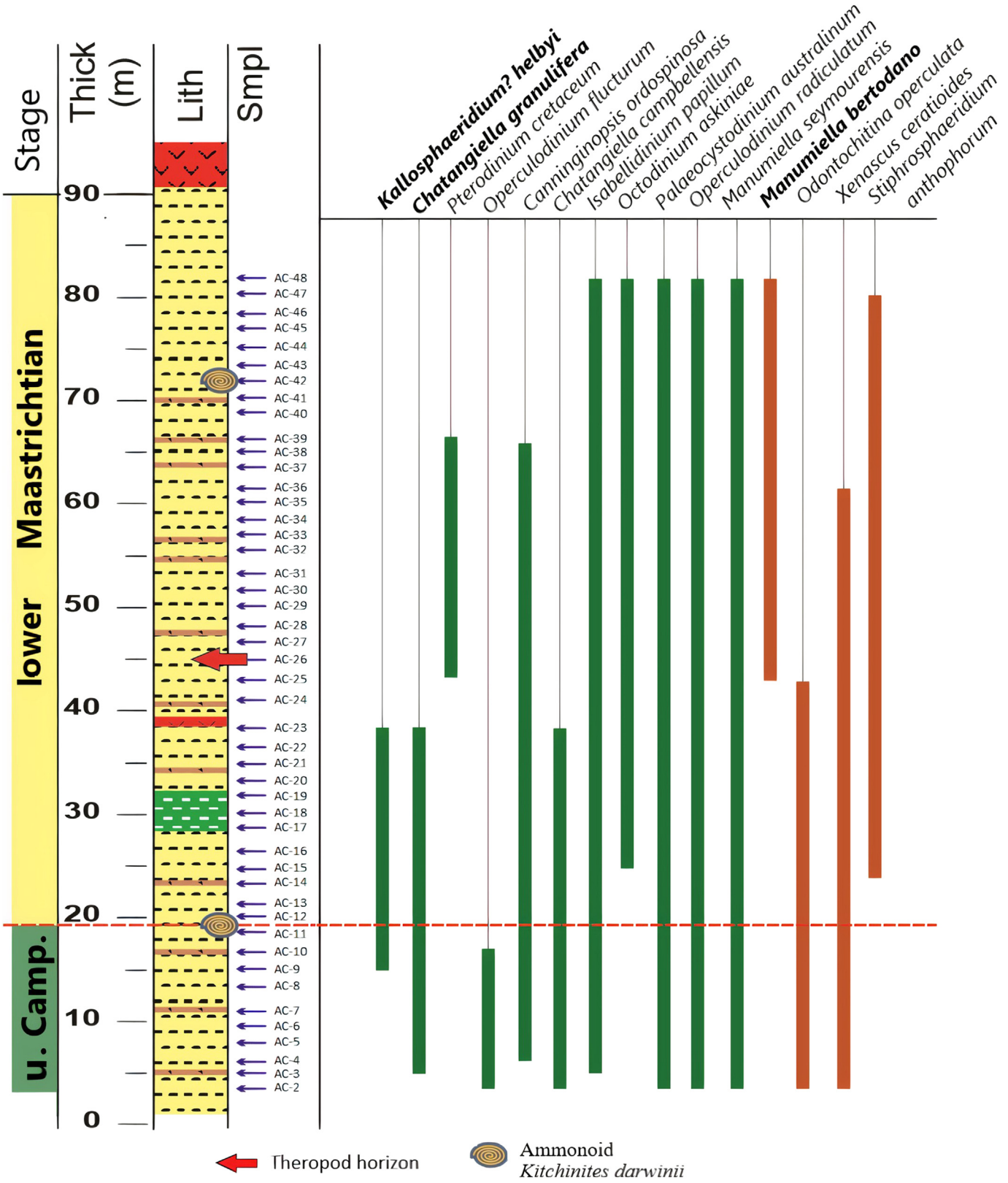


**Fig. 7.** Stratigraphic distribution of the marker species in the section studied. *Kallosphaeroidiun? helby*, *Chatangiella granulifera*, and *Manumiella bertodano* correspond to the probable upper Campanian–lower Maastrichtian boundary, as indicated by the dashed red line in between samples AC-12 and AC-11. (For interpretation of the references to color in this figure legend, the reader is referred to the Web version of this article.)

Although there is the possibility of reworking, we did not find any evidence of Maastrichtian age, below the ammonoid *K. darwinii* about 20 m base to outcrop.

The present study includes all the samples collected across the section, and the presence of *Manumiella bertodano* from sample AC-25 (42.92 m) to sample AC-48 (81.73 m) confirms the reported *Manumiella* sp. cf. *M. bertodano* by di Pasquo and Martin (2013), in the upper part of section (50–73 m). This taxon has been documented as appearing in the late Maastrichtian (<72.1 Ma). However, *M. bertodano* in The Naze's upper layers, together with *Odontochitina operculata*, *Xenascus ceratiodes*, and *Stiphrosphaeridium anthophorum,* indicates that its stratigraphic range reaches the early Maastrichtian in an interval not younger than 70 Ma. The rest of the upper strata species have younger stratigraphical records, extending to the Cretaceous–Paleogene boundary (~66 Ma). Therefore, the sedimentary column was deposited during the latest Campanian to early Maastrichtian. These data agree with the biostratigraphic analysis established by di Pasquo and Martin (2013), in which the ammonoid *Kitchinites darwinii* indicates a Maastrichtian age down to sample AC-12 (20.12 m). However, we propose a late Campanian age for the lower part of the section due to the higher occurrences of the late Campanian marker species *Kallosphaeridium? helbyi* and *Chatangiella granulifera*. We propose to locate the probable Campanian–Maastrichtian limit between the samples AC-12 and AC-11 (red line; Fig. 7). The presence of several specimens of *K.? helbyi* and *C. granulifera* above the lowest appearance of *K. darwinii* is interpreted as reworking.

### 4.3. Paleoenvironments and paleoecology

The sediments' hemipelagic character and the predominance of dinoflagellate cysts in the palynological assemblages indicate deposition in marine environments for the studied section at The Naze as proposed by di Pasquo and Martin (2013).

The monotonous mixture of silts and clays to fine sands with biogenic pelagic material represents mostly inner to middle neritic facies (0–100 m) (Fig. 8). However, the deeper environment at ca. 28–35 m, where silty claystones prevail, indicates a slight transgressive tendency to middle to outer neritic (100–200 m), below normal-weather wave base. In contrast, at ca. 45 m, the remains of theropod dinosaurs and decapod crustaceans (di Pasquo and Martin, 2013) indicate a shallower interval, probably inner neritic (0–50 m).

We count 17 autotrophic species and 32 heterotrophic ones. We use these groups to try and understand the response of the dinoflagellate cyst assemblages to paleoclimatic or paleoceanographic changes. The groups with greater richness are not the groups with higher concentrations in the studied samples, neither considering the taxonomic groupings nor the trophic strategies. The Peridiniales include 27 species representing 55.10% of the total, but their mean concentration is 39.46%. In comparison, the Gonyaulacales represent 53.44% of the total concentration, with only 14 species representing 28.57% of the species observed (Table 2). Similarly, heterotrophic taxa represent 65.30% of the species counted, while they only reach 46.15% of the concentration, in contrast to the 53.85% of autotrophic taxa (Fig. 8).

As for the concentrations per gram of sediment (cyst/g sed), the average of total dinoflagellate = 1508.88 cyst/g sed; autotrophic = 892.27 cyst/g sed, and heterotrophic = 616.62 cyst/g sed, and the average Heterotrophic–Autotrophic Index = 0.54 (Fig. 8). Autotrophic taxa dominate most of the lower Maastrichtian interval, with higher concentration values. In contrast, the upper Campanian values are dominated by heterotrophic and have lower total concentration values.

Mean diversity at The Naze H = 3.35, which is considered a relatively diverse average, considering that this index fluctuates in general between 0 and 5. The upper Campanian interval dominated by heterotrophic has a high diversity in general, while the lower Maastrichtian interval, with two autotrophic intervals (samples AC-23 to AC-27 and AC-32 to AC-48), presents less diversity. High diversity values correspond to high values of the H–A Index. Among the frequency of terrestrial and marine taxa presented by di Pasquo and Martin (2013), we also noticed the abundant presence of angiosperms, especially the genus *Nothofagidites.*

## 5. Discussions

Diagenetic changes can diminish the recovery of less resistant heterotrophic taxa (Zonneveld et al., 2008). However, the higher concentrations in our samples also have higher H/A values. Therefore, we consider that changes in the dinoflagellate cyst assemblages reflect changes in paleoproductivity. Without geochemical data of the strata, mainly Vanadium or Molybdenum (Tribovillard et al., 2004; Bennett and Canfield, 2020), we cannot define the sediments' redox environment. However, given the unvarying lithology shown (Fig. 2), the probability of diagenetic dilution of heterotrophic taxa is similar throughout the section studied. Therefore, we use cysts' concentrations per gram of sediment from the Late Cretaceous strata from The Naze to interpret their productivity and compare them with similar data from living assemblages. This interpretation is a relative and non-linear comparison with recent age analyses, recognizing the changing nature of the record, as well as uncertainty about the trophic behavior during the Late Cretaceous caused by the selectivity of the fossil record dinoflagellates.

These values compare marine productivity in equivalent terms, even though scales in time and location might differ, data on cyst concentrations in Recent sediments from highly productive locations are are reported in cysts/g sed values. For example, in the central Gulf of California, the high primary productivity in the Guaymas Basin is reflected in concentrations of up to 31,000 cyst/g sed, whereas concentrations in the northern Gulf of California range between 4500 and ~17,000 cyst/g sed (Pospelova et al., 2008). These concentrations of marine productivity are comparable to other areas with upwelling and high productivity, such as West Africa ~130 to ~65,600 cyst/g sed (Bouimetarhan et al., 2009), the Chilean continental margin ~525 to ~ 100,750 cyst/g sed (Verleye and Louwye, 2010) and the Northeast Pacific ~ 100 to 35,000 cyst/g sed (Pospelova et al., 2008).

Comparing the concentration values found in The Naze (Mean = 1508.9 cyst/g sed; Max = 17,456.9 cyst/g sed) and those from Recent sediments (Table 4) allows the James Ross Basin could be to be classified as a basin with moderate to high productivity. Albeit one where autotrophic dinoflagellate taxa dominated, thus registering a different quality from that reported for many actual basins, where heterotrophs usually are dominant.

Oceanographic and biological conditions most likely differed during the Late Cretaceous. One important factor is the phytoplankton's taxonomic composition since biomarker data, and the fossil record of diatom frustules indicate that these microalgae were a minor component in the oceans until the end of the Eocene, approximately 35–40 Ma (Cermeño, 2016). In the Late Cretaceous, the Aut dinoflagellates most probably occupied the niche within the trophic structure that now diatoms have. We interpret that the predominance of Aut dinoflagellate cysts in The Naze means they were the leading primary producers. In our samples, the autotrophic “Areoligeraceans” and “Cribroperidinioids” took the role that diatoms have in today's trophic chain. The absence of siliceous cement in the samples supports this interpretation.

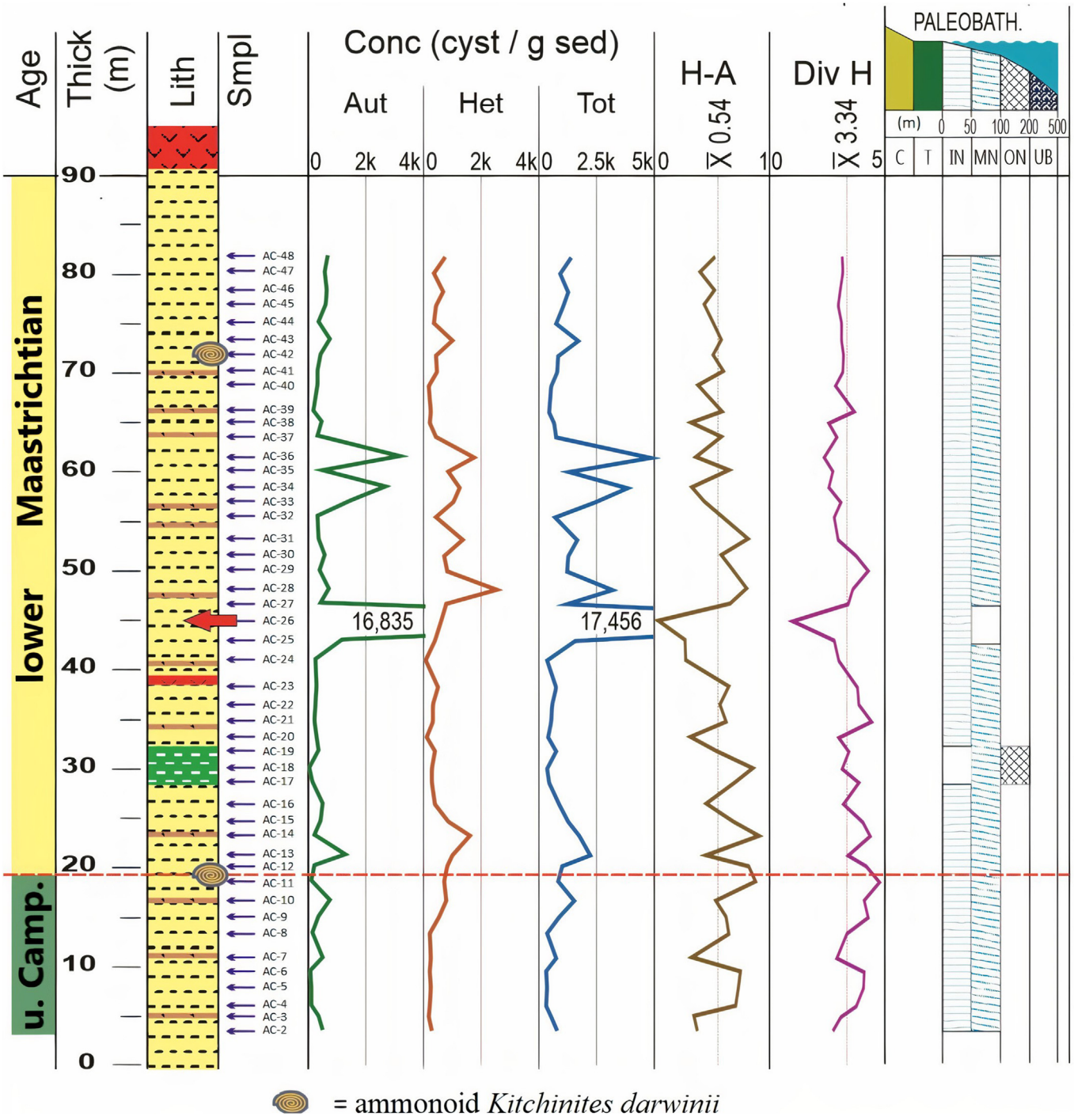


**Fig. 8.** Age; Lith = lithology; Smpl = sample; sums of groups indicated by PCA (∑A1, ∑A2, ∑A3), and concentration (Cyst/g sed) of total dinoflagellate cyst taxa; H–A = Het–Aut Index; Shannon diversity index = Div H of dinoflagellate cysts, and paleobathymetry (PALEOBATH) interpreted for The Naze section. The red arrow indicates the position of the theropod horizon in the section, and the dashed red line indicates the position of the probable upper Campanian–lower Maastrichtian boundary in the section. Paleobathimetry: C = continental, T = transitional, IN = inner neritic, MN = middle neritic, ON = outside neritic, UB = upper bathyal. (For interpretation of the references to color in this figure legend, the reader is referred to the Web version of this article.)

Diversity and the ecosystem's related stability depend on biological and environmental factors (Hutchinson, 1959). The stability can vary due to changes in the environmental components such as sea surface temperature, direction, wind speed, and nutrients. From this perspective, intervals with more diversity are the more stable and probably respond to the system's appropriate amount of nutrients. Intervals with a predominance of Het taxa coincide with higher diversity values (H > 3.34; samples AC-2 to AC-23 and AC-27 to AC-32). Despite these intervals showing variable diversity, brief but significant paleoenvironmental changes are suggested. On the contrary, an interval with a more stable tendency (H ≈ 3.34) occurs at the top of the section (samples AC-32 to AC-48), with probably constant small-scale paleoenvironmental fluctuations.

Consequently, the low diversity interval (samples AC-23 to AC-27) with a high concentration of Aut (16,835 cyst/g sed) is

**Table 4**
Average values of concentration data of dinoflagellate cysts (cst/g sed) in our samples, the Oligocene–Miocene La Purisima Basin (LPB; Toscano-Cepeda and Helenes, 2021) and some Recent basins around Baja California (Magdalena; Castañeda Quezada, 2016), San Lazaro (Serrano Mejía, 2016; Pérez Rodríguez, 2016), and Pescadero (Flores-Trujillo et al., 2009). The age of the Recent basins corresponds to calendar years, while the age of LPB and The Naze are in Ma. HET = heterotrophic taxa; AUT = autotrophic taxa; TOT = total taxa; Het/Aut = HET/HET + AUT.

| | | Concentration Cysts (cyst/g sed) | | | |
|---|---|---|---|---|---|
| Basins (Age) | | HET | AUT | TOT | Het/Aut |
| Magdalena (1908–2008) | Average | 168.9 | 31.8 | 200.7 | 0.79 |
| Pescadero (1905–1995) | | 812.39 | 293.46 | 1105.85 | 0.71 |
| San Lázaro (1965–2009) | | 1488.70 | 70.9 | 1599.60 | 0.9 |
| LPB early Mio (28–23 Ma) | | 232.71 | 615.2 | 847.91 | 0.36 |
| LPB -late Oli (21.17–23 Ma) | | 34.34 | 168.81 | 203.15 | 0.43 |
| The Naze (~72.6 – ~70.6 Ma) | | 616.6 | 892.3 | 1508.9 | 0.5 |

considered unstable in the ecosystem, although with highly favorable conditions marked by the acme of the Aut *C. muderongense*. This proliferation was probably related to an increase in nutrients, probably associated with the terrigenous influx, as indicated by the theropod dinosaurs' presence in the same stratigraphic interval (di Pasquo and Martin, 2013).

From the continental point of view, the presence of pollen of the Fusca group (*Nothofagidites saraensis*) is observed, indicating conditions of moderate humidity and temperate climate (Barreda, 1997), associated with ice-free zones (Haller, 2002). These conditions support the proposed cool to temperate, frost-free climate hypothesis for the study area at the age interval assigned here (Dettmann, 1986, 1989; Askin, 1990a, 1990b; Dettmann et al., 1992; Crame, 1992; Hill and Scriven, 1995; Miller et al., 2008; Bastos et al., 2013). The dinoflagellate *Chatangiella* in the lower part of the section (upper Campanian?) also indicates a temperate climate. This genus formed part of the warm temperate Malloy suite and the colder boreal Mc Intyre suite (Lentin and Williams, 1980) and was reported in Brazil's southeast (Arai et al., 2000) associated with relatively warmer sea surface temperatures. In contrast, the genus *Manumiella*, which predominates in the upper part (early Maastrichtian), is related to high latitudes (Askin, 1999) and is associated with lower temperatures. The stratigraphic distribution of these genera indicates cooling but without evidence of glaciation at or near The Naze Peninsula. Icy conditions would prevent the presence of both *Chatangiella* and the *Fusca* group in the stratigraphic record.

## 6. Conclusions

The proposed stage assignment for this study section is based on the last appearance (LO) of dinoflagellates cysts *Kallosphaeridium? helbyi, Chatangiella granulifera, Odontochitina operculata, Xenascus ceratiodes,* and *Stiphrosphaeridium anthophorum,* along with the first appearance (FO) of *Pterodinium cretaceum, Manumiella seymourensis, Palaeocystodinium australinum, Canninginopsis ordospinosa, Operculodinium flucturum, Operculodinium radiculatum, Chatangiella campbellensis, Isabelidinium papillum, Octodinium askiniae,* and *Manumiella bertodano,* is upper Campanian–lower Maastrichtian. The James Ross Basin is considered a moderate to high productivity basin (1508.9 cyst/g sed). In the Late Cretaceous, the predominance of Aut dinoflagellate cysts in The Naze Peninsula means that they were the main primary producers, and cool to temperate, frost-free climate hypotheses are proposed for the study area in the age range assigned here.

## Data availability

Data will be made available on request.

## Acknowledgments

Thanks to CONACYT – CICESE, for financial support to the first author through a master's degree scholarship between 2015 and 2017. Professor Wiesława Radmacher (Polish Academy of Sciences) for her comments about redaction. Thanks to MSc Mariletty Calderón (Málaga University) for her support in editing images. The author wishes to thank Dr. James Riding for his review and feedback. Thanks, are also due to Dr. Eduardo Koutsoukos for constructive comments on the manuscript. We thank the second reviewer for the useful comments that improved the paper.

## References

Amenábar, C.R., Caramés, A., Adamonis, S., Doldan, A., Maceiras, G., Concheyro, A., 2019. Mesozoic and Cenozoic microbiotas from eastern Antarctic Peninsula: adaptation to a changing palaeoenvironment. Advances in Polar Science 30 (3), 165–185. https://doi.org/10.13679/j.advps.2019.0017.

Arai, M., Neto, J.B., Lana, C.C., Pedrão, E., 2000. Cretaceous dinoflagellate provincialism in Brazilian marginal basins. Cretaceous Research 21 (2–3), 351–366. https://doi.org/10.1006/cres.2000.021.

Askin, R.A., 1988. Campanian to Paleocene palynological succession of Seymour and adjacent islands, northeastern Antarctic Peninsula. Geological Society of America Memoirs 169, 131–154. https://doi.org/10.1130/MEM169-p131.

Askin, R.A., 1990a. Campanian to Paleocene spore and pollen assemblages of Seymour Island, Antarctica. Review of Palaeobotany and Palynology 65 (1–4), 105–113. https://doi.org/10.1016/0034-6667(90)90061-M.

Askin, R.A., 1990b. Cryptogam spores from the upper Campanian and Maastrichtian of Seymour Island, Antarctica. Micropaleontology 141–156. https://doi.org/10.2307/1485498.

Askin, R.A., 1999. *Manumiella seymourensis* new species, a stratigraphically significant dinoflagellate cyst from the Maastrichtian of Seymour Island, Antarctica. Journal of Paleontology 73 (3), 373–379. https://doi.org/10.1017/S0022336000027888.

Askin, R.A., Elliot, D.H., Stilwell, J.D., Zinsmeister, W.J., 1991. Stratigraphy and paleontology of Campanian and Eocene sediments, Cockburn Island, Antarctic Peninsula. Journal of South American Earth Sciences 4 (1–2), 99–117. https://doi.org/10.1016/0895-9811(91)90021-C.

Barreda, V.D., 1997. Palinoestratigrafía de la Formación San Julián en el área de Playa La Mina (provincia de Santa Cruz), Oligoceno de la cuenca austral. Ameghiniana 34 (3), 283–294.

Bastos, B.L.i, Dutra, T.L., Wilberger, T.P., Trevisan, C., 2013. Uma Flora do final do Cretáceo na ilha Nelson, Ilhas Shetland do Sul, Península Antártica. Revista Brasileira de Paleontologia 16 (3), 441–464. https://doi.org/10.4072/rbp.2013.3.06.

Bennett, W.W., Canfield, D.E., 2020. Redox-sensitive trace metals as paleoredox proxies: a review and analysis of data from modern sediments. Earth-Science Reviews 204, 103175. https://doi.org/10.1016/j.earscirev.2020.103175.

Benninghoff, W.S., 1962. Calculation of pollen and spore density in sediments by addition of exotic pollen in known quantities. Polles Spores 4, 332.

Bouimetarhan, I., Dupont, L., Schefuß, E., Mollenhauer, G., Mulitza, S., Zonneveld, K., 2009. Palynological evidence for climatic and oceanic variability off NW Africa during the late Holocene. Quaternary Research 72 (2), 188–197. https://doi.org/10.1016/j.yqres.2009.05.003.

Bowman, V.C., Francis, J.E., Riding, J.B., Hunter, S.J., Haywood, A.M., 2012. A latest Cretaceous to earliest Paleogene dinoflagellate cyst zonation from Antarctica, and implications for phytoprovincialism in the high southern latitudes. Review of Palaeobotany and Palynology 171, 40–56. https://doi.org/10.1016/j.revpalbo.2011.11.004.

Bowman, V.C., Francis, J.E., Riding, J.B., 2013a. Late Cretaceous winter sea ice in Antarctica? Geology 41 (12), 1227–1230. https://doi.org/10.1130/G34891.1.

Bowman, V.C., Riding, J.B., Francis, J.E., Crame, J.A., Hannah, M.J., 2013b. The taxonomy and palaeobiogeography of small chorate dinoflagellate cysts from the Late Cretaceous to Quaternary of Antarctica. Palynology 37 (1), 151–169. https://doi.org/10.1080/01916122.2012.750898.

Bowman, V.C., Francis, J.E., Askin, R.A., Riding, J.B., Swindles, G.T., 2014. Latest Cretaceous–earliest Paleogene vegetation and climate change at the high southern latitudes: palynological evidence from Seymour Island, Antarctic Peninsula. Palaeogeography, Palaeoclimatology, Palaeoecology 408, 26–47. https://doi.org/10.1016/j.palaeo.2014.04.018.

Brinkhuis, H., Sengers, S., Sluijs, A., Warnaar, J., Williams, G.L., 2003. Latest Cretaceous to earliest Oligocene, and quaternary dinoflagellate cysts from ODP Site 1172, East Tasman Plateau. In: Exon, N.F., Kennett, J.P., Malone, M.J. (Eds.), Proc. ODP, Sci. Results, 189, pp. 1–48.

Bujak, J.P., Williams, G.L., 1985. Mesozoic and Cenozoic dinoflagellates. Plankton stratigraphy 847–965.

Calabozo, F.M., Strelin, J., Orihashi, Y., Sumino, H., Keller, R.A., 2015. Volcano-ice-sea interaction in the Cerro Santa Marta area, northwest James Ross Island, Antarctic Peninsula. Journal of Volcanology and Geothermal Research 297, 89e108. https://doi.org/10.1016/j.jvolgeores.2015.03.011.

Case, J.A., Martin, J.E., Reguero, M., 2007. A dromaeosaur from the Maastrichtian of James Ross Island and the Late Cretaceous dinosaur fauna, vol. 83. US Geological Survey and the National Academies. https://doi.org/10.3133/of2007-1047.srp083. USGS OF-2007-1047. Short Research Paper.

Castañeda Quezada, J.R., 2016. 100 años de Dinoflagelados y cambios Paleoceanográficos en Cuenca Magdalena, Baja California Sur. Tesis de Maestría en Ciencias. Centro de Investigación Científica y de Educación Superior de Ensenada, Baja California, p. 77.

Cermeño, P., 2016. The geological story of marine diatoms and the last generation of fossil fuels. Perspectives in Phycology 53–60. https://doi.org/10.1127/pip/2016/0050.

Crame, J.A., Pirrie, D., Riding, J.B., Thomson, M.R.A., 1991. Campanian-Maastrichtian (Cretaceous) stratigraphy of the James Ross Island area, Antarctica. Journal of the Geological Society of London 148, 1125–1140. https://doi.org/10.1144/gsjgs.148.6.1125.

Crame, J.A., 1992. Late Cretaceous palaeoenvironments and biotas: an Antarctic perspective. Antarctic Science 4 (4), 371–382. https://doi.org/10.1017/S0954102092000555.

Crame, J.A., McArthur, J.M., Pirrie, D., Riding, J.B., 1999. Strontium isotope correlation of the basal Maastrichtian Stage in Antarctica to the European and U.S. biostratigraphic schemes. Journal of the Geological Society 156 (5), 957–964. https://doi.org/10.1144/gsjgs.156.5.0957.

Crame, J.A., Francis, J.E., Cantrill, D.J., Pirrie, D., 2004. Maastrichtian stratigraphy of Antarctica. Cretaceous Research 25 (3), 411–423. https://doi.org/10.1016/j.cretres.2004.02.002.

Davey, R.J., 1969. Non-calcareous microplankton from the Cenomanian of England, northern France and North America, Part I. Bulletin of the British Museum (Natural History) Geology 17, 103–180.

Dettmann, M.E., 1986. Early Cretaceous palynoflora of subsurface strata correlative with the Koonwarra Fossil Bed, Victoria. Memoir of the Association of Australasian Palaeontologists 3, 79–110.

Dettmann, M.E., 1989. Antarctica: Cretaceous Cradle of Austral Temperate Rainforests? Geological Society, London, Special Publications, pp. 89–105. https://doi.org/10.1144/GSL.SP.1989.047.01.08.

Dettmann, M.E., Molnar, R.E., Douglas, J.G., Burger, D., Fielding, C., Clifford, H.T., et al., 1992. Australian Cretaceous terrestrial faunas and floras: biostratigraphic and biogeographic implications. Cretaceous Research 13 (3), 207–262. https://doi.org/10.1016/0195-6671(92)90001-7.

di Pasquo, M., Martin, J.E., 2013. Palynoassemblages associated with a theropod dinosaur from the Snow Hill Island formation (lower Maastrichtian) at the Naze, James Ross Island, Antarctica. Cretaceous Research 45, 135–154. https://doi.org/10.1016/j.cretres.2013.07.008.

Ely, R.C., Case, J.A., 2019. Phylogeny of a new gigantic paravian (Theropoda; coelurosauria; maniraptora) from the upper cretaceous of James Ross island, Antarctica. Cretaceous Research 101, 1–16. https://doi.org/10.1016/j.cretres.2019.04.003.

Fensome, R.A., 2019. The Lentin and Williams Index of Fossil Dinoflagellates, 2019 edn. In: AASP Contribution Series. (50).

Flores-Trujillo, J.G., Helenes, J., Herguera, J.C., Orellana-Cepeda, E., 2009. Palynological record (1483–1994) of *Gymnodinium catenatum* in Pescadero Basin, southern Gulf of California, Mexico. Marine Micropaleontology 73 (1), 80–89. https://doi.org/10.1016/j.marmicro.2009.06.009.

Friedrich, O., Herrle, J.O., Wilson, P.A., Cooper, M.J., Erbacher, J., Hemleben, C., 2009. Early Maastrichtian carbon cycle perturbation and cooling event: Implications from the South Atlantic Ocean. Paleoceanography 24 (PA2211), 1–14. https://doi.org/10.1029/2008PA001654.

Gradstein, F.M., Ogg, J.G., Schmitz, M., Ogg, G. (Eds.), 2012. The geologic time scale 2012. Elsevier.

Guerra, R.M., Concheyro, A., Lees, J., Fauth, G., Carvalho, M.A., Ramos, R.R.C., 2015. Calcareous nannofossils from the Santa Marta Formation (Upper Cretaceous), northern James Ross Island, Antarctic Peninsula. Cretaceous Research 56, 550e562. https://doi.org/10.1016/j.cretres.2015.06.009.

Haller, M.J., 2002. Geología y Recursos Naturales de Santa Cruz. In: Relatorio del 15 Congreso Geológico Argentino, El Calafate, pp. 1–925.

Harland, R., 1973. Dinoflagellate cysts and acritarchs from the Bearpaw Formation (Upper Campanian) of southern Alberta, Canada. Palaeontology 16 (pt 4), 665–706.

Helenes, J., Somoza, D., 1999. Palynology and sequence stratigraphy of the Cretaceous of eastern Venezuela. Cretaceous Research 20 (4), 447–463. https://doi.org/10.1006/cres.1999.0160.

Hill, R.S., Scriven, L.J., 1995. The angiosperm-dominated woody vegetation of Antarctica: a review. Review of Palaeobotany and Palynology 86 (3–4), 175–198. https://doi.org/10.1016/0034-6667(94)00149-E.

Hutchinson, G.E., 1959. Homage to Santa Rosalia or why are there so many kinds of animals? The American Naturalist 93 (870), 145–159.

Lentin, J.K., Williams, G.L., 1980. Dinoflagellate Provincialism with Emphasis on Campanian peridiniaceans. In: American Association of Stratigraphic Palynologists, Contributions Series, vol. 7, pp. 1–47 pl.1.

Linnert, C., Robinson, S.A., Lees, J.A., Páerez-Rodríguez, I., Hugh, C., Jenkyns, H.C., et al., 2018. Did Late Cretaceous cooling trigger the Campaniane–Maastrichtian Boundary Event? Newsletters on Stratigraphy 51 (2), 145–166. https://doi.org/10.1127/nos/2017/0310.

Maher, L.J., 1981. Statistics for microfossil concentration measurements employing samples spiked with marker grains. Review of Palaeobotany and Palynology 32 (2–3), 153–191. https://doi.org/10.1016/0034-6667(81)90002-6.

Mao, S., Mohr, B.A., 1992. Late Cretaceous dinoflagellate cysts (?Santonian-Maestrichtian) from the southern Indian Ocean (hole 748C). In: Proceedings of the Ocean Drilling Program, Scientific Results, vol. 120, pp. 307–341.

Martin, J.E., Sawyer, J.F., Reguero, M., Case, J.A., 2007. Occurrence of a young elasmosaurid plesiosaur skeleton from the Late Cretaceous (Maastrichtian) of Antarctica. In: Antarctica: A Keystone in a Changing World, Online Proceedings of the 10th International Symposium of Antarctic Earth Sciences, United States Geological Survey, Open-File Report, vol. 1047. https://doi.org/10.3133/of2007-1047.srp066.

Mertens, K.N., Verhoeven, K., Verleye, T., Louwye, S., Amorim, A., Ribeiro, S., et al., 2009. Determining the absolute abundance of dinoflagellate cysts in recent marine sediments: the *Lycopodium* marker-grain method put to the test. Review of Palaeobotany and Palynology 157 (3), 238–252. https://doi.org/10.1016/j.revpalbo.2009.05.004.

Mertens, K.N., Bradley, L.R., Takano, Y., Mudie, P.J., Marret, F., Aksu, A.E., et al., 2012. Quantitative estimation of Holocene surface salinity variation in the Black Sea using dinoflagellate cyst process length. Quaternary Science Reviews 39, 45–59. https://doi.org/10.1016/j.quascirev.2012.01.026.

Miller, K.G., Wright, J.D., Katz, M.E., Browning, J.V., Cramer, B.S., Wade, B.S., et al., 2008. A view of Antarctic ice-sheet evolution from sea-level and deep-sea isotope changes during the Late Cretaceous–Cenozoic. Antarctica: A Keystone in a Changing World 55–70.

Olivero, E.B., 2012. Sedimentary cycles, ammonite diversity and palaeoenvironmental changes in the Upper Cretaceous Marambio Group, Antarctica. Cretaceous Research 34, 348–366. https://doi.org/10.1016/j.cretres.2011.11.015.

Pérez Rodríguez, J.C., 2016. Registro palinológico en sedimentos laminados de la cuenca San Lázaro, Baja California Sur y su relación con cambios paleoceanográficos y paleoclimáticos de 1965 a 1988. Tesis de Maestría en Ciencias. Centro de Investigación Científica y de Educación Superior de Ensenada, Baja California, p. 62.

Piovesan, E.K., Correia Filho, O.J., Melo, R.M., Lacerda, L.D., Dos Santos, R.O., Pinheiro, A.P., et al., 2020. The Campanian–Maastrichtian interval at The Naze, James Ross Island, Antarctica: microbiostratigraphic and paleoenvironmental study. Cretaceous Research 120, 104725. https://doi.org/10.1016/j.cretres.2020.104725.

Pirrie, D., Crame, J.A., Riding, J.B., 1991. Late Cretaceous stratigraphy and sedimentology of Cape Lamb, Vega Island, Antarctica. Cretaceous Research 12, 227–258. https://doi.org/10.1016/0195-6671(91)90036-C.

Pirrie, D., Crame, J.A., Lomas, S.A., Riding, J.B., 1997. Late Cretaceous stratigraphy of the Admiralty Sound region, James Ross Basin, Antarctica. Cretaceous Research 18 (1), 109–137. https://doi.org/10.1006/cres.1996.0052.

Pospelova, V., de Vernal, A., Pedersen, T.F., 2008. Distribution of dinoflagellate cysts in surface sediments from the northeastern Pacific Ocean (43–25 N) in relation to sea-surface temperature, salinity, productivity and coastal upwelling. Marine Micropaleontology 68 (1), 21–48. https://doi.org/10.1016/j.marmicro.2008.01.008.

Reichart, G.J., Brinkhuis, H., 2003. Late Quaternary *Protoperidinium* cysts as indicators of paleoproductivity in the northern Arabian Sea. Marine Micropaleontology 49 (4), 303–315. https://doi.org/10.1016/S0377-8398(03)00050-1.

Roncaglia, L., Field, B.D., Raine, J.I., Schiøler, P., Wilson, G.J., 1999. Dinoflagellate biostratigraphy of Piripauan-Haumurian (Upper Cretaceous) sections from northeast South Island, New Zealand. Cretaceous Research 20 (3), 271–314. https://doi.org/10.1006/cres.1999.0153.

Serrano Mejía, C.G., 2016. Registro palinológico en sedimentos laminados de la cuenca San Lázaro, Baja California sur y su relación con cambios paleoceanográficos y paleoclimáticos de 1988 a 2009. Tesis de Maestría en Ciencias. Centro de Investigación Científica y de Educación Superior de Ensenada, Baja California, p. 46.

Shannon, C.E., Weaver, W., 1949. The Mathematical Theory of Communications. Univ. Illinois Press, Urbana.

Slimani, H., Louwye, S., Toufiq, A., Verniers, J., De Coninck, J., 2008. New dinoflagellate cyst species from Cretaceous/Palaeogene boundary deposits at Ouled Haddou, south-eastern Rif, Morocco. Cretaceous Research 29 (2), 329–344. https://doi.org/10.1016/j.cretres.2007.06.003.

Slimani, H., Mahboub, I., Toufiq, A., Jbari, H., Chakir, S., Tahiri, A., 2019. Bartonian to Priabonian dinoflagellate cyst biostratigraphy and paleoenvironments of the M'karcha section in the Southern Tethys margin (Rif Chain, Northern Morocco). Marine Micropaleontology 153, 101785. https://doi.org/10.1016/j.marmicro.2019.101785.

Smith, S.W., 1992. Microplankton from the Cape Lamb Member, López de Bertodano Formation (Upper Cretaceous), Cape Lamb, Vega Island. Antarctic Science 4 (3), 337–353. https://doi.org/10.1017/S095410209200049X.

Thorn, V.C., Riding, J.B., Francis, J.E., 2009. The Late Cretaceous dinoflagellate cyst Manumiella—Biostratigraphy, systematics, and palaeoecological signals in Antarctica. Review of Palaeobotany and Palynology 156 (3), 436–448. https://doi.org/10.1016/j.revpalbo.2009.04.009.

Toscano-Cepeda, A.E., Helenes, J., 2021. Oligocene–Miocene Dinoflagellate Cysts from the San Gregorio Formation, La Purísima Area, Baja California Sur, Mexico. Palynology 46 (1), 1–20. https://doi.org/10.1080/01916122.2021.1927880.

Tribovillard, N., Ramdani, A., Trentesaux, A., 2004. Controls on organic accumulation in Late Jurassic shales of Northwestern Europe as inferred from trace-metal geochemistry. Bulletin de la Societe Geologique de France 175 (5), 491–506. https://doi.org/10.2113/175.5.491.

Verleye, T.J., Louwye, S., 2010. Late Quaternary environmental changes and latitudinal shifts of the Antarctic Circumpolar Current as recorded by dinoflagellate cysts from offshore Chile (41°S). Quaternary Science Reviews 29 (7), 1025–1039. https://doi.org/10.1016/j.quascirev.2010.01.009.

Vink, A., Zonneveld, K.A., Willems, H., 2000. Organic-walled dinoflagellate cysts in western equatorial Atlantic surface sediments: distributions and their relation to environment. Review of Palaeobotany and Palynology 112 (4), 247–286. https://doi.org/10.1016/S0034-6667(00)00046-4.

Wilson, G.J., 1984. New Zealand Late Jurassic to Eocene dinoflagellate biostratigraphy-a summary. Newsletters on stratigraphy 104–117. https://doi.org/10.1127/nos/13/1984/104.

Wood, G.D., Gabriel, A.M., Lawson, J.C., 1996. Palynological techniques processing and microscopy. In: Jansonius, J., McGregor, D.C. (Eds.), Palynology: Principles and Applications, vol. 1, pp. 29–50.

Zonneveld, K.A., Versteegh, G., Kodrans-Nsiah, M., 2008. Preservation and organic chemistry of Late Cenozoic organic-walled dinoflagellate cysts: a review. Marine Micropaleontology 68 (1–2), 179–197. https://doi.org/10.1016/j.marmicro.2008.01.015.

## Appendix A. Supplementary data

Supplementary data to this article can be found online at https://doi.org/10.1016/j.cretres.2022.105367.